

Isospin quartic term in the kinetic energy of neutron-rich nucleonic matter

Bao-Jun Cai and Bao-An Li*

Department of Physics and Astronomy, Texas A&M University-Commerce, Commerce, Texas 75429-3011, USA

(Received 3 March 2015; revised manuscript received 11 June 2015; published 2 July 2015)

The energy of a free gas of neutrons and protons is well known to be approximately isospin parabolic with a negligibly small quartic term of only 0.45 MeV at the saturation density of nuclear matter $\rho_0 = 0.16 \text{ fm}^{-3}$. Using an isospin-dependent single-nucleon momentum distribution including a high (low) momentum tail (depletion) with its shape parameters constrained by recent high-energy electron scattering and medium-energy nuclear photodisintegration experiments as well as the state-of-the-art calculations of the deuteron wave function and the equation of state of pure neutron matter near the unitary limit within several modern microscopic many-body theories, we show for the first time that the kinetic energy of interacting nucleons in neutron-rich nucleonic matter has a significant quartic term of $7.18 \pm 2.52 \text{ MeV}$. Such a large quartic term has broad ramifications in determining the equation of state of neutron-rich nucleonic matter using observables of nuclear reactions and neutron stars.

DOI: [10.1103/PhysRevC.92.011601](https://doi.org/10.1103/PhysRevC.92.011601)

PACS number(s): 21.65.Ef, 24.10.Ht, 21.65.Cd

Introduction. To determine the equation of state (EOS) of isospin-asymmetric nuclear matter (ANM) has been a longstanding goal in the fields of both nuclear physics and astrophysics [1]. Usually one uses the so-called empirical parabolic law for the energy per nucleon, i.e., $E(\rho, \delta) = E_0(\rho) + E_{\text{sym}}(\rho)\delta^2 + O(\delta^4)$, where $\rho = \rho_n + \rho_p$ and $\delta = (\rho_n - \rho_p)/\rho$ are the nucleon density and isospin asymmetry of the system in terms of the neutron and proton densities ρ_n and ρ_p , respectively. The isospin quadratics of the ANM EOS has been verified to high accuracies from symmetric ($\delta = 0$) up to pure neutron ($\delta = 1$) matter by most of the available nuclear many-body theories using various interactions, see, e.g., Ref. [2]. Nevertheless, it has been shown consistently in a number of studies that for some physical quantities relevant to understanding the properties of neutron stars, such as the proton fraction at β equilibrium, the core-crust transition density, and the critical density for the direct URCA process to happen, even a very small coefficient $E_{\text{sym},4}(\rho)$ of the isospin quartic term in the EOS can make a big difference [3].

Here we concentrate on examining the isospin quadratics of the kinetic EOS. For many purposes in both nuclear physics and astrophysics, such as simulating heavy-ion collisions [4] and determining critical formation densities of different charge states of Δ resonances in neutron stars [5], one has to know separately the kinetic and potential parts of the EOS. While neither any fundamental physical principle nor the empirical parabolic law of the EOS requires the kinetic and potential parts of the EOS to be quadratic in δ individually, in practice especially in most phenomenological models the free Fermi gas (FFG) EOS is often used for the kinetic part and then the generally less known potential EOS is explored by comparing model predictions with experimental data. It is well known that the FFG model predicts a kinetic symmetry energy of $E_{\text{sym}}^{\text{kin}}(\rho_0) \approx 12.3 \text{ MeV}$ and a negligibly small quartic term of $E_{\text{sym},4}^{\text{kin}}(\rho_0) = E_{\text{sym}}^{\text{kin}}(\rho_0)/27 \approx 0.45 \text{ MeV}$ at $\rho_0 = 0.16/\text{fm}^3$. However, nuclear interactions, in particular the short-range repulsive core

and tensor force, lead to a high (low) momentum tail (depletion) in the single-nucleon momentum distribution above (below) the nucleon Fermi surface [6–9]. Much progress has been made recently both theoretically and experimentally in quantifying especially the nucleon high momentum tails (HMTs) in ANM, see, e.g., Refs. [10–14]. In this work, using isospin-dependent nucleon HMTs constrained by recent high-energy electron scattering and medium-energy nuclear photodisintegration experiments as well as the state-of-the-art calculations of the deuteron wave function and the EOS of pure neutron matter (PNM) near the unitary limit within several modern microscopic many-body theories, we show that the kinetic ANM EOS has a significant quartic term of $E_{\text{sym},4}^{\text{kin}}(\rho_0) = 7.18 \pm 2.52 \text{ MeV}$, which is about 16 times the FFG model prediction.

Isospin dependence of single-nucleon momentum distribution with a high momentum tail in neutron-rich matter. Guided by well-known predictions of microscopic nuclear many-body theories, see, e.g., reviews in Ref. [15], and recent experimental findings [10–13], we describe the single-nucleon momentum distribution in ANM using

$$n_{\mathbf{k}}^J(\rho, \delta) = \begin{cases} \Delta_J + \beta_J I(|\mathbf{k}|/k_F^J), & 0 < |\mathbf{k}| < k_F^J, \\ C_J (k_F^J/|\mathbf{k}|)^4, & k_F^J < |\mathbf{k}| < \phi_J k_F^J. \end{cases} \quad (1)$$

Here, $J = n, p$ is the isospin index, $k_F^J = k_F(1 + \tau_3^J \delta)^{1/3}$ is the transition momentum [13] where $k_F = (3\pi^2 \rho/2)^{1/3}$ and $\tau_3^n = +1$, $\tau_3^p = -1$. The main features of $n_{\mathbf{k}}^J(\rho, \delta)$ are depicted in Fig. 1. The Δ_J measures the depletion of the Fermi sphere at zero momentum with respect to the FFG model prediction while β_J is the strength of the momentum dependence $I(|\mathbf{k}|/k_F^J)$ [16–18] of the depletion near the Fermi surface. The jump Z_F^J of the momentum distribution at k_F^J , namely, the “renormalization function,” contains information about the nucleon effective E-mass and its isospin dependence [19]. Specifically, $Z_F^J = n_{k_F^J-0}^J - n_{k_F^J+0}^J = M/M_E^{J,*}$, where $M_E^{J,*}/M \equiv [1 - \partial V/\partial \omega]^{-1}$ with V and ω being the real part of the single-particle potential and energy [6,20], respectively.

*Bao-An.Li@tamuc.edu

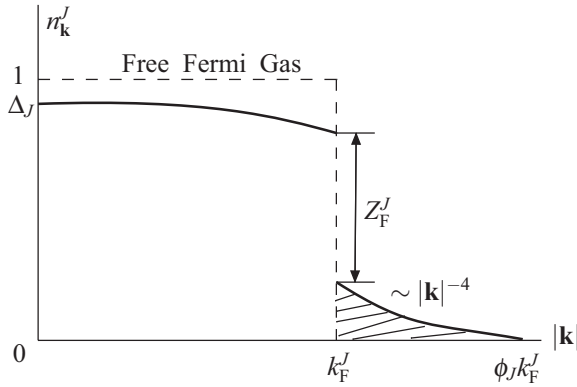


FIG. 1. Sketch of the single-nucleon momentum distribution with a high momentum tail.

The amplitude C_J and cutoff coefficient ϕ_J determine the fraction of nucleons in the HMT via

$$x_J^{\text{HMT}} = 3C_J \left(1 - \frac{1}{\phi_J}\right). \quad (2)$$

The normalization condition $[2/(2\pi)^3] \int_0^\infty n_{\mathbf{k}}^J(\rho, \delta) d\mathbf{k} = \rho_J = (k_F^J)^3/3\pi^2$ requires that only three of the four parameters, i.e., β_J , C_J , ϕ_J , and Δ_J , are independent. Here we choose the first three as independent and determine the Δ_J from

$$\Delta_J = 1 - \frac{3\beta_J}{(k_F^J)^3} \int_0^{k_F^J} I\left(\frac{k}{k_F^J}\right) k^2 dk - 3C_J \left(1 - \frac{1}{\phi_J}\right). \quad (3)$$

Suggested by the finding within the self-consistent Green's function (SCGF) theory [21] and the Brueckner-Hartree-Fock (BHF) theory [22] that the depletion Δ_J has an almost linear dependence on δ in the opposite directions for neutrons and protons, we expand all four parameters in the form $Y_J = Y_0(1 + Y_1^J \delta)$. Then, the total kinetic energy per nucleon in ANM

$$E^{\text{kin}}(\rho, \delta) = \frac{1}{\rho} \frac{2}{(2\pi)^3} \sum_{J=n,p} \int_0^{\phi_J k_F^J} \frac{\mathbf{k}^2}{2M} n_{\mathbf{k}}^J(\rho, \delta) d\mathbf{k} \quad (4)$$

would obtain a linear term in δ of the form

$$\begin{aligned} E_1^{\text{kin}}(\rho) &= \frac{3}{5} \frac{k_F^2}{2M} \left[\frac{5}{2} C_0 \phi_0 (\phi_1^n + \phi_1^p) \right. \\ &\quad + \frac{5}{2} C_0 (\phi_0 - 1) (C_1^n + C_1^p) + \frac{1}{2} \Delta_0 (\Delta_1^n + \Delta_1^p) \\ &\quad \left. + \frac{5\beta_0 (\beta_1^n + \beta_1^p)}{2k_F^5} \int_0^{k_F} I\left(\frac{k}{k_F}\right) k^4 dk \right], \quad (5) \end{aligned}$$

where M is the nucleon mass. To ensure that $E_1^{\text{kin}}(\rho)$ vanishes as required by the neutron-proton exchange symmetry of the EOS, we require that $\Delta_1^n = -\Delta_1^p$, $\beta_1^n = -\beta_1^p$, $C_1^n = -C_1^p$, and $\phi_1^n = -\phi_1^p$, i.e., more compactly $Y_J = Y_0(1 + Y_1 \tau_3^J \delta)$.

Constraining the parameters of the single-nucleon momentum distribution. It is well known that the nucleon HMT from deuteron to infinite nuclear matter scales, see, e.g., Refs. [23–27], leading to constant per nucleon inclusive (e, e') cross sections for heavy nuclei with respect to the deuteron for the Bjorken scaling parameter x_B between about 1.5 and 1.9;

see, e.g., Ref. [28] for a recent review. Systematic analyses of these inclusive experiments and data from exclusive two-nucleon knockout reactions induced by high-energy electrons or protons have firmly established that the HMT fraction in symmetric nuclear matter (SNM) is about $x_{\text{SNM}}^{\text{HMT}} = 28\% \pm 4\%$ and that in PNM it is about $x_{\text{PNM}}^{\text{HMT}} = 1.5\% \pm 0.5\%$ [12–14,29].

The $C/|k|^4$ shape of the HMT for both SNM and PNM is strongly supported by recent theoretical and experimental findings. The HMT for deuteron from variational many-body calculations using several modern nuclear forces decreases as $|k|^{-4}$ within about 10% and in quantitative agreement with that from analyzing the $d(e, e' p)$ cross section in directions where the final state interaction suffered by the knocked-out proton is small [12]. The extracted magnitude $C_{\text{SNM}} = C_0$ of the HMT in SNM at ρ_0 is $C_0 \approx 0.15 \pm 0.03$ [12] (properly rescaled considering the factor of 2 difference in the adopted normalizations of $n_{\mathbf{k}}$ here and that in Refs. [12,29]). Rather remarkably, a very recent evaluation of medium-energy photonuclear absorption cross sections has also presented clear and independent evidence for the $C/|k|^4$ behavior of the HMT and extracted a value of $C_0 \approx 0.172 \pm 0.007$ [10] for SNM at ρ_0 in very good agreement with that found in Ref. [12]. In the following, we use $C_0 \approx 0.161 \pm 0.015$ from taking the average of the above two constraints. With this C_0 and the value of $x_{\text{SNM}}^{\text{HMT}}$ given earlier, the HMT cutoff parameter in SNM is determined to be $\phi_0 = (1 - x_{\text{SNM}}^{\text{HMT}}/3C_0)^{-1} = 2.38 \pm 0.56$.

Very interestingly, the $1/|k|^4$ behavior of the HMT nucleons is identical to that in two-component (spin-up and -down) cold fermionic atoms first predicted by Tan [30] and then quickly verified experimentally [31]. Tan's general prediction is for all two-component fermion systems having an s -wave contact interaction with a scattering length a much larger than the interparticle distance d which has to be much longer than the interaction range r_e . At the unitary limit when $|k_F a| \rightarrow \infty$, Tan's prediction is universal for all fermion systems. Since the HMT in nuclei and SNM is known to be dominated by the tensor force induced neutron-proton pairs with the $a \approx 5.4$ fm and $d \approx 1.8$ fm at ρ_0 , as noted in Refs. [10,12], Tan's stringent conditions for unitary fermions is obviously not satisfied in normal nuclei and SNM. The observed identical $1/|k|^4$ behavior of the HMTs in nuclei and cold atoms may have some deeper physical reasons deserving further investigations. Indeed, a very recent study on $A(e, e' p)$ and $A(e, e' pp)$ scattering has shown that the majority of the short-range correlation (SRC)-susceptible n - p pairs are in the 3S_1 state [32]. On the other hand, because of the unnaturally large neutron-neutron scattering length $a_{nn}(^1S_0) = -18.8$ fm, it is known that PNM is closer to the unitary limit [33]. The EOS of PNM can thus be expanded as [34]

$$\begin{aligned} E_{\text{PNM}}(\rho) &\simeq \frac{3}{5} \frac{(k_F^{\text{PNM}})^2}{2M} \left[\xi - \frac{\zeta}{k_F^{\text{PNM}} a_{nn}} \right. \\ &\quad \left. - \frac{5\nu}{3(k_F^{\text{PNM}} a_{nn})^2} \right], \quad (6) \end{aligned}$$

where $k_F^{\text{PNM}} = 2^{1/3} k_F$ is the transition momentum in PNM, $\xi \approx 0.4 \pm 0.1$ is the Bertsch parameter [35], and $\zeta \approx \nu \approx 1$ are two universal constants [36].

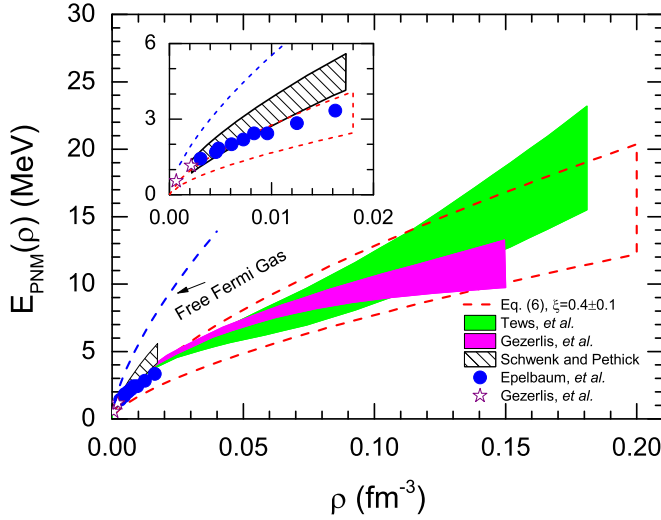


FIG. 2. (Color online) EOS of PNM obtained from Eq. (6) (dashed red band) and that from next-leading-order (NLO) lattice calculation [37] (blue solid points), chiral perturbative theories [38] (green band), quantum Monte Carlo simulations (QMC) [39,40] (magenta band and purple stars), and effective field theory [33].

Shown in Fig. 2 is a comparison of the EOS of PNM obtained from Eq. (6) (dashed red band) with several state-of-the-art calculations using modern microscopic many-body theories. At densities less than about 0.01 fm^{-3} , as shown in the inset, Eq. (6) is consistent with the prediction by the effective field theory [33]. In the range of 0.01 fm^{-3} to about 0.02 fm^{-3} , it has some deviations from predictions in Ref. [33] but agrees very well with the NLO lattice simulations [37]. At higher densities up to about ρ_0 , it overlaps largely with predictions by the chiral perturbation theories [38] and the quantum Monte Carlo simulations [39,40]. In addition, recent studies on the spin-polarized neutron matter within the chiral effective field theory including two-, three-, and four-neutron interactions indicate that properties of PNM are similar to those of the unitary Fermi gas at least up to ρ_0 far beyond the scattering-length regime of $\rho \lesssim \rho_0/100$ [41]. Overall, the above comparison and studies clearly justify the use of Eq. (6) to calculate the PNM EOS up to about ρ_0 .

Both the HMT and EOS can be experimentally measured independently and calculated simultaneously within the same model. Tan has proven in great detail that the two are directly

related by the so-called adiabatic sweep theorem [30]. It is valid for any two-component Fermi systems under the same conditions as Eq. (6) near the unitary limit. For PNM, it can be written as

$$C_n^{\text{PNM}}(k_F^{\text{PNM}})^4 = -4\pi M \frac{d(\rho E_{\text{PNM}})}{d(a^{-1})}. \quad (7)$$

While the results shown in Fig. 2 justify the use of Eq. (6) for the EOS of PNM up to about ρ_0 , indeed, to the best of our knowledge there is currently no proof that Eq. (7) is also valid in the same density range as Eq. (6). Thus, it would be very interesting to examine the validity range of Eq. (7) using the same models as those used to calculate the EOS. In this work, we assume that Eqs. (6) and (7) are both valid in the same density range. Then, the strength of the HMT in PNM can be readily obtained as

$$C_n^{\text{PNM}} \approx 2\zeta/5\pi + 4\nu/[3\pi k_F^{\text{PNM}} a_{\text{nn}}(^1S_0)] \approx 0.12. \quad (8)$$

Noticing that $C_n^{\text{PNM}} = C_0(1 + C_1)$, we can then infer that $C_1 = -0.25 \pm 0.07$ with the C_0 given earlier. Next, after inserting the values of $x_{\text{PNM}}^{\text{HMT}}$ and C_n^{PNM} into Eq. (2), the high momentum cutoff parameter for PNM is determined to be $\phi_n^{\text{PNM}} \equiv \phi_0(1 + \phi_1) = (1 - x_{\text{PNM}}^{\text{HMT}}/3C_n^{\text{PNM}})^{-1} = 1.04 \pm 0.02$. It is not surprising that the ϕ_n^{PNM} is very close to unity since only about 1.5% of the neutrons are in the HMT in PNM. Subsequently, using the ϕ_0 determined earlier, we get $\phi_1 = -0.56 \pm 0.10$.

The two parameters β_0 and β_1 in $\beta_J = \beta_0(1 + \beta_1 \tau_3^J \delta)$ depend on the function $I(|\mathbf{k}|/k_F^J)$ which is still model dependent. To minimize the model assumptions and evaluate the dominating terms in the kinetic EOS, in the following we shall first use a momentum-independent depletion of the Fermi sea as in most studies in the literature. The HMT parameters C_J and ϕ_J evaluated above remain the same. Then, we examine the maximum correction to each term in the kinetic EOS by using the largest values of β_0 and β_1 allowed and a typical function $I(|\mathbf{k}|/k_F^J)$. Not surprisingly, the corrections are all small.

Isospin dependence of kinetic EOS of ANM. The kinetic EOS can be expanded in δ as

$$E^{\text{kin}}(\rho, \delta) = E_0^{\text{kin}}(\rho) + E_{\text{sym}}^{\text{kin}}(\rho)\delta^2 + E_{\text{sym},4}^{\text{kin}}(\rho)\delta^4 + O(\delta^6). \quad (9)$$

The coefficients evaluated from Eq. (4) using the $n_{\mathbf{k}}^J(\rho, \delta)$ in Eq. (1) with $\beta_J = 0$ are

$$E_0^{\text{kin}}(\rho) = \frac{3}{5} E_F(\rho) \left[1 + C_0 \left(5\phi_0 + \frac{3}{\phi_0} - 8 \right) \right], \quad (10)$$

$$E_{\text{sym}}^{\text{kin}}(\rho) = \frac{1}{3} E_F(\rho) \left[1 + C_0(1 + 3C_1) \left(5\phi_0 + \frac{3}{\phi_0} - 8 \right) + 3C_0\phi_1 \left(1 + \frac{3}{5}C_1 \right) \left(5\phi_0 - \frac{3}{\phi_0} \right) + \frac{27C_0\phi_1^2}{5\phi_0} \right], \quad (11)$$

$$E_{\text{sym},4}^{\text{kin}}(\rho) = \frac{1}{81} E_F(\rho) \left[1 + C_0(1 - 3C_1) \left(5\phi_0 + \frac{3}{\phi_0} - 8 \right) + 3C_0\phi_1(9C_1 - 1) \left(5\phi_0 - \frac{3}{\phi_0} \right) + \frac{81C_0\phi_1^2(9\phi_1^2 - 9C_1\phi_1 - 15\phi_1 + 15C_1 + 5)}{5\phi_0} \right]. \quad (12)$$

In the FFG where there is no HMT, $\phi_0 = 1$, $\phi_1 = 0$, and thus $5\phi_0 + 3/\phi_0 - 8 = 0$, the above expressions reduce naturally to the well-known results of $E_0^{\text{kin}}(\rho) = 3E_F(\rho)/5$, $E_{\text{sym}}^{\text{kin}}(\rho) = E_F(\rho)/3$, and $E_{\text{sym},4}^{\text{kin}}(\rho)/E_{\text{sym}}^{\text{kin}}(\rho) = 1/27$, where $E_F(\rho) = k_F^2/2M$ is the Fermi energy.

For the interacting nucleons in ANM with the momentum distribution and its parameters given earlier, we found that $E_0^{\text{kin}}(\rho_0) = 40.45 \pm 8.15$ MeV, $E_{\text{sym}}^{\text{kin}}(\rho_0) = -13.90 \pm 11.54$ MeV, and $E_{\text{sym},4}^{\text{kin}}(\rho_0) = 7.19 \pm 2.52$ MeV, respectively. Compared to the corresponding values for the FFG, it is seen that the isospin-dependent HMT increases significantly the average kinetic energy $E_0^{\text{kin}}(\rho_0)$ of SNM but decreases the kinetic symmetry energy $E_{\text{sym}}^{\text{kin}}(\rho_0)$ of ANM to a negative value qualitatively consistent with the findings of several recent studies of the kinetic EOS considering short-range nucleon-nucleon correlations using both phenomenological models and microscopic many-body theories [42–47]. However, it was completely unknown before if the empirical isospin parabolic law is still valid for the kinetic EOS of ANM when the isospin-dependent HMTs are considered. Very surprisingly and interestingly, our calculations here show clearly that it is broken seriously. More quantitatively, the ratio $|E_{\text{sym},4}^{\text{kin}}(\rho_0)/E_{\text{sym}}^{\text{kin}}(\rho_0)|$ is about $52\% \pm 26\%$, which is much larger than the FFG value of 3.7%. We also found that the large quartic term is mainly due to the isospin dependence of the HMT cutoff described by the ϕ_1 parameter. For example, by artificially setting $\phi_1 = 0$, we obtain $E_{\text{sym}}^{\text{kin}}(\rho_0) = 14.68 \pm 2.80$ MeV and $E_{\text{sym},4}^{\text{kin}}(\rho_0) = 1.12 \pm 0.27$ MeV which are all close to their FFG values.

Considering short-range nucleon-nucleon correlations but assuming that the isospin parabolic approximation is still valid, some previous studies have evaluated the kinetic symmetry energy $E_{\text{sym}}^{\text{kin}}$ by taking the difference between the kinetic energies of PNM and SNM, i.e., subtracting the E_0^{kin} from $E_{\text{PNM}}^{\text{kin}}$. This actually approximately equals $E_{\text{sym}}^{\text{kin}}(\rho_0) + E_{\text{sym},4}^{\text{kin}}(\rho_0) = -6.71 \pm 9.11$ MeV in our current work. This value is consistent quantitatively with the $E_{\text{sym}}^{\text{kin}}(\rho_0)$ found in Ref. [29] using the parabolic approximation.

Corrections due to the momentum-dependent depletion of the Fermi sea. To estimate corrections due to the momentum dependence of the depletion very close to the Fermi surface, i.e., a finite β_J , we consider a widely used single-nucleon momentum distribution parametrized in Ref. [25] based on calculations using many-body theories. For $|\mathbf{k}| \lesssim 2 \text{ fm}^{-1}$, it goes like $\sim e^{-\alpha|\mathbf{k}|^2}$ with $\alpha \approx 0.12 \text{ fm}^2$. At ρ_0 since $\alpha k_F^2 \approx 0.21$, $e^{-\alpha|\mathbf{k}|^2} \approx 1 - \alpha|\mathbf{k}|^2 + O(|\mathbf{k}|^4)$ is a good approximation in the range of $0 < |\mathbf{k}| < k_F^J$. Thus, we adopt a quadratic function $I(|\mathbf{k}|/k_F^J) = (|\mathbf{k}|/k_F^J)^2$. The constants in the parametrization of Ref. [25] are absorbed into our parameters Δ_J and β_J . Then Eq. (3) gives us $\Delta_J = 1 - 3\beta_J/5 - 3C_J(1 - 1/\phi_J)$. Specifically, we have $\beta_0 = (5/3)[1 - \Delta_0 - 3C_0(1 - \phi_0^{-1})] = (5/3)[1 - \Delta_0 - x_{\text{SNM}}^{\text{HMT}}]$ for SNM. Then using the predicted value of $\Delta_0 \approx 0.88 \pm 0.03$ [9,22,23] and the experimental value of $x_{\text{SNM}}^{\text{HMT}} \approx 0.28 \pm 0.04$, the value of β_0 is estimated to be about -0.27 ± 0.08 . Similarly, the condition $\beta_J = \beta_0(1 + \beta_1 \tau_3^J \delta) < 0$, i.e., $n_{\mathbf{k}}^J$ is a decreasing function of momentum towards k_F^J , indicates that $|\beta_1| \leq 1$.

First of all, a finite value of β_J is expected to affect the “renormalization function” Z_F^J . For SNM, we have $Z_F^0 = 1 + 2\beta_0/5 - C_0 - x_{\text{SNM}}^{\text{HMT}} = 0.45 \pm 0.07$ (0.56 ± 0.04) in the presence (absence) of β_0 . For ANM, however, the Z_F^J depends on the less constrained value of β_1 . It is worth noting that the latter also determines the neutron-proton effective E-mass splitting which has significant effects on isovector observables in heavy-ion collisions [48], and a study is underway to further constrain the value of β_1 using data from heavy-ion reactions.

Contributions from a finite β_J to the first three terms of the kinetic EOS are

$$\delta E_0^{\text{kin}}(\rho) = \frac{3}{5} E_F(\rho_0) \frac{4\beta_0}{35}, \quad (13)$$

$$\delta E_{\text{sym}}^{\text{kin}}(\rho) = \frac{1}{3} E_F(\rho_0) \frac{4\beta_0(1 + 3\beta_1)}{35}, \quad (14)$$

$$\delta E_{\text{sym},4}^{\text{kin}}(\rho) = \frac{1}{81} E_F(\rho_0) \frac{4\beta_0(1 - 3\beta_1)}{35}. \quad (15)$$

With the largest magnitude of $\beta_0 = -0.35$, we examine in Fig. 3 the corrections to the $E_{\text{sym}}^{\text{kin}}(\rho_0)$ and $E_{\text{sym},4}^{\text{kin}}(\rho_0)$ as functions of β_1 in its full range allowed. In this case the maximum effects of the finite β_J are revealed. It is seen that the correction on the $E_{\text{sym},4}^{\text{kin}}(\rho_0)$ is negligible while the correction on the $E_{\text{sym}}^{\text{kin}}(\rho_0)$ is less than 2 MeV. Considering the corrections due to the finite β_0 and β_1 and their uncertainties, we finally obtain $E_0^{\text{kin}}(\rho_0) = 39.77 \pm 8.13$ MeV, $E_{\text{sym}}^{\text{kin}}(\rho_0) = -14.28 \pm 11.59$ MeV, and $E_{\text{sym},4}^{\text{kin}}(\rho_0) = 7.18 \pm 2.52$ MeV. We notice here that the δ^6 term was also consistently evaluated and was found to be negligibly small at ρ_0 .

Summary and discussion. In summary, using an isospin-dependent single-nucleon momentum distribution including a high (low) momentum tail (depletion) with its shape parameters constrained by the latest results of several relevant experiments and the state-of-the-art predictions of modern microscopic many-body theories, we found for the first time that the kinetic EOS of interacting nucleons in ANM is not parabolic in isospin asymmetry. It has a significant

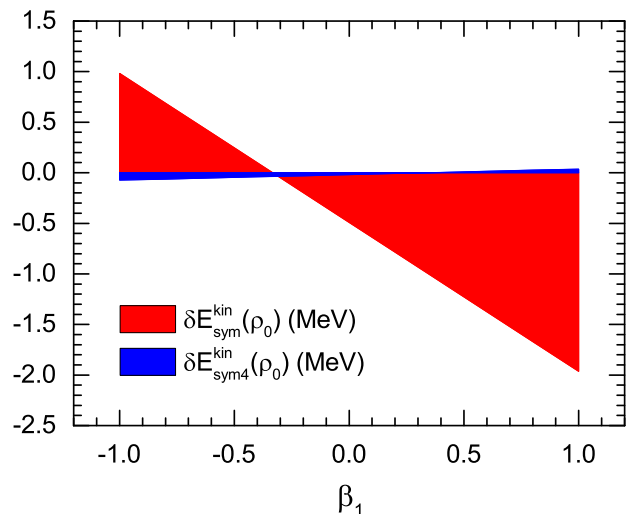


FIG. 3. (Color online) Corrections to the $E_{\text{sym}}^{\text{kin}}(\rho_0)$ and $E_{\text{sym},4}^{\text{kin}}(\rho_0)$ as functions of β_1 with $\beta_0 = -0.35$.

quartic term of 7.18 ± 2.52 MeV while its quadratic term is -14.28 ± 11.60 MeV at saturation density of nuclear matter.

To this end, it is necessary to point out the limitations of our approach and a few physical implications of our findings. Since we fixed the parameters of the nucleon momentum distribution [Eq. (1)] by using experimental data and/or model calculations at the saturation density, the possible density dependence of these parameters is not explored in this work. The density dependence of the various terms in the kinetic EOS is thus only due to that of the Fermi energy as shown in Eqs. (10)–(12). In this limiting case, the slope of the kinetic symmetry energy, i.e., $L^{\text{kin}} = 3\rho_0 \partial E_{\text{sym}}^{\text{kin}}(\rho) / \partial \rho |_{\rho=\rho_0} = -27.81 \pm 23.08$ MeV while that of the FFG is about 25.04 MeV.

The SRC-reduced kinetic symmetry energy with respect to the FFG prediction has been found to affect significantly not only our understanding about the origin of the symmetry energy but also several isovector observables, such as the free neutron/proton and π^-/π^+ ratios in heavy-ion collisions [29,49,50]. However, to our best knowledge, an investigation on the possible effects of a large isospin quartic term on heavy-ion collisions has never been done, while its effects on the properties of neutron stars have been studied extensively [3]. Of course, effects of the quartic and quadratic terms should be studied together within the same approach. To extract from nuclear reactions and neutron stars information about the EOS of neutron-rich matter, people often parametrize the EOS as a sum of the kinetic energy of a FFG and a potential energy involving unknown parameters up to the isospin-quadratic term only. Our findings in this work indicate

that it is important to include the isospin-quartic term in both the kinetic and potential parts of the EOS. Moreover, to accurately extract the completely unknown isospin-quartic term $E_{\text{sym},4}^{\text{pot}}(\rho)\delta^4$ in the potential EOS it is important to use the kinetic EOS of quasiparticles with reduced kinetic symmetry energy and an enhanced quartic term due to the isospin dependence of the HMT. Most relevant to the isovector observables in heavy-ion collisions, such as the neutron-proton ratio and differential flow, is the nucleon isovector potential. Besides the so-called Lane potential $\pm 2\rho E_{\text{sym}}^{\text{pot}}(\rho)\delta$ where the $E_{\text{sym}}^{\text{pot}}(\rho)$ is the potential part of the symmetry energy and the \pm sign is for neutrons/protons, the $E_{\text{sym},4}^{\text{pot}}(\rho)\delta^4$ term contributes an additional isovector potential $\pm 4\rho E_{\text{sym},4}^{\text{pot}}(\rho)\delta^3$. In neutron-rich systems besides neutron stars, such as nuclear reactions induced by rare isotopes and peripheral collisions between two heavy nuclei having thick neutron skins, the latter may play a significant role in understanding the isovector observables or extracting the sizes of neutron skins of the nuclei involved. We plan to study the effects of the isospin-quartic term in the EOS in heavy-ion collisions using the isospin-dependent transport model [4] in the near future.

Acknowledgments. We thank L. W. Chen, O. Hen, X. H. Li, W. G. Newton, E. Piasezky, A. Rios, I. Vidaña, and L. B. Weinstein for helpful discussions. This work is supported in part by the US National Science Foundation under Grant No. PHY-1068022 and the US Department of Energy, Office of Science, under Award No. DE-SC0013702.

-
- [1] *Topical Issue on Nuclear Symmetry Energy*, edited by B. A. Li, A. Ramos, G. Verde, and I. Vidaña, Eur. Phys. J. A **50**, No. 2 (Springer, 2014).
- [2] I. Bombaci and U. Lombardo, *Phys. Rev. C* **44**, 1892 (1991).
- [3] O. Sjöberg, *Nucl. Phys. A* **222**, 161 (1974); A. W. Steiner, *Phys. Rev. C* **74**, 045808 (2006); C. Providência, L. Brito, S. S. Avancini, D. P. Menezes, and Ph. Chomaz, *ibid.* **73**, 025805 (2006); C. Ducoin, J. Margueron, and P. Chomaz, *Nucl. Phys. A* **809**, 30 (2008); J. Xu *et al.*, *Astrophys. J.* **697**, 1549 (2009); B. J. Cai and L. W. Chen, *Phys. Rev. C* **85**, 024302 (2012); W. M. Seif and D. N. Basu, *ibid.* **89**, 028801 (2014).
- [4] B. A. Li, L. W. Chen, and C. M. Ko, *Phys. Rep.* **464**, 113 (2008).
- [5] B. J. Cai, F. J. Fattoyev, B. A. Li, and W. G. Newton, *Phys. Rev. C* (to be published), [arXiv:1501.01680](https://arxiv.org/abs/1501.01680).
- [6] A. B. Migdal, *Sov. Phys. JETP* **5**, 333 (1957).
- [7] H. A. Bethe, *Ann. Rev. Nucl. Part. Sci.* **21**, 93 (1971).
- [8] V. R. Pandharipande and S. C. Pieper, *Phys. Rev. C* **45**, 791 (1992).
- [9] V. R. Pandharipande, I. Sick, and P. K. A. deWitt Huberts, *Rev. Mod. Phys.* **69**, 981 (1997).
- [10] R. Weiss, B. Bazak, and N. Barnea, *Phys. Rev. Lett.* **114**, 012501 (2015).
- [11] R. Weiss, B. Bazak, and N. Barnea, [arXiv:1503.07047](https://arxiv.org/abs/1503.07047).
- [12] O. Hen, L. B. Weinstein, E. Piasezky, G. A. Miller, M. Sargsian, and Y. Sagi, [arXiv:1407.8175](https://arxiv.org/abs/1407.8175).
- [13] O. Hen *et al.*, *Science* **346**, 614 (2014).
- [14] K. S. Egiyan *et al.*, *Phys. Rev. Lett.* **96**, 082501 (2006); E. Piasezky, M. Sargsian, L. Frankfurt, M. Strikman, and J. W. Watson, *ibid.* **97**, 162504 (2006); R. Shneur *et al.*, *ibid.* **99**, 072501 (2007); R. Subedi *et al.*, *Science* **320**, 1476 (2008); L. B. Weinstein *et al.*, *Phys. Rev. Lett.* **106**, 052301 (2011); I. Korover *et al.*, *ibid.* **113**, 022501 (2014).
- [15] A. N. Antonov, P. E. Hodgson, and I. Zh. Petkov, *Nucleon Momentum and Density Distribution in Nuclei* (Clarendon, Oxford, 1988).
- [16] V. A. Belykov, *Sov. Phys. JETP* **13**, 850 (1961).
- [17] W. Czyz and K. Gottfried, *Nucl. Phys.* **21**, 676 (1960).
- [18] R. Sartor and C. Mahaux, *Phys. Rev. C* **21**, 1546 (1980).
- [19] J. P. Jeukenne, A. Lejeune, and C. Mahaux, *Phys. Rep.* **25**, 83 (1976); C. Mahaux, P. F. Bortignon, R. A. Broglia, and C. H. Dasso, *ibid.* **120**, 1 (1985).
- [20] J. M. Luttinger, *Phys. Rev.* **119**, 1153 (1960).
- [21] A. Rios, A. Polls, and W. H. Dickhoff, *Phys. Rev. C* **79**, 064308 (2009).
- [22] P. Yin, J. Y. Li, P. Wang, and W. Zuo, *Phys. Rev. C* **87**, 014314 (2013).
- [23] S. Fantoni and V. R. Pandharipande, *Nucl. Phys. A* **427**, 473 (1984).
- [24] S. C. Pieper, R. B. Wiringa, and V. R. Pandharipande, *Phys. Rev. C* **46**, 1741 (1992).
- [25] C. Ciofi degli Atti and S. Simula, *Phys. Rev. C* **53**, 1689 (1996).
- [26] D. B. Day *et al.*, *Phys. Rev. C* **40**, 1011 (1989).

- [27] C. Ciofi degli Atti, E. Pace, and G. Salmè, *Phys. Rev. C* **43**, 1155 (1991).
- [28] J. Arrington, D. W. Higinbotham, G. Rosner, and M. Sargsian, *Prog. Part. Nucl. Phys.* **67**, 898 (2012).
- [29] O. Hen, B. A. Li, W. J. Guo, L. B. Weinstein, and E. Piasetzky, *Phys. Rev. C* **91**, 025803 (2015).
- [30] S. N. Tan, *Ann. Phys. (NY)* **323**, 2952 (2008); **323**, 2971 (2008); **323**, 2987 (2008).
- [31] J. T. Stewart, J. P. Gaebler, T. E. Drake, and D. S. Jin, *Phys. Rev. Lett.* **104**, 235301 (2010); E. D. Kuhnle *et al.*, *ibid.* **105**, 070402 (2010).
- [32] C. Colle *et al.*, [arXiv:1503.06050](https://arxiv.org/abs/1503.06050).
- [33] A. Schwenk and C. J. Pethick, *Phys. Rev. Lett.* **95**, 160401 (2005).
- [34] G. A. Baker, Jr., *Phys. Rev. C* **60**, 054311 (1999); H. Heiselberg, *Phys. Rev. A* **63**, 043606 (2001); K. M. O'Hara *et al.*, *Science* **298**, 2179 (2002); T. L. Ho, *Phys. Rev. Lett.* **92**, 090402 (2004); S. Y. Chang, V. R. Pandharipande, J. Carlson, and K. E. Schmidt, *Phys. Rev. A* **70**, 043602 (2004); G. E. Astrakharchik, J. Boronat, J. Casulleras, and S. Giorgini, *Phys. Rev. Lett.* **93**, 200404 (2004); F. Werner, L. Tarruell, and Y. Castin, *Eur. Phys. J. B* **68**, 401 (2009).
- [35] M. Randeria, W. Zwerger, and M. Zwierlein, in *The BCS-BES Crossover and The Unitary Fermi Gas*, edited by W. Zwerger (Springer, Berlin, 2012).
- [36] A. Bulgac and G. F. Bertsch, *Phys. Rev. Lett.* **94**, 070401 (2005).
- [37] E. Epelbaum, H. Krebs, D. Lee, and Ulf-G. Meissner, *Eur. Phys. A* **40**, 199 (2009).
- [38] I. Tews, T. Krüger, K. Hebeler, and A. Schwenk, *Phys. Rev. Lett.* **110**, 032504 (2013); T. Krüger, I. Tews, K. Hebeler, and A. Schwenk, *Phys. Rev. C* **88**, 025802 (2013).
- [39] A. Gezerlis *et al.*, *Phys. Rev. Lett.* **111**, 032501 (2013).
- [40] A. Gezerlis and J. Carlson, *Phys. Rev. C* **81**, 025803 (2010).
- [41] T. Krüger, K. Hebeler, and A. Schwenk, *Phys. Lett. B* **744**, 18 (2015).
- [42] C. Xu and B. A. Li, [arXiv:1104.2075](https://arxiv.org/abs/1104.2075); C. Xu, A. Li, and B. A. Li, *J. Phys. Conf. Ser.* **420**, 012090 (2013).
- [43] I. Vidaña, A. Polls, and C. Providência, *Phys. Rev. C* **84**, 062801(R) (2011).
- [44] A. Lovato, O. Benhar, S. Fantoni, A. Yu. Illarionov, and K. E. Schmidt, *Phys. Rev. C* **83**, 054003 (2011).
- [45] A. Carbone, A. Polls, and A. Rios, *Eur. Phys. Lett.* **97**, 22001 (2012).
- [46] A. Rios, A. Polls, and W. H. Dickhoff, *Phys. Rev. C* **89**, 044303 (2014).
- [47] A. Carbone, A. Polls, C. Providência, A. Rios, and I. Vidaña, *Eur. Phys. A* **50**, 13 (2014).
- [48] B. A. Li and L. W. Chen, *Mod. Phys. Lett. A* **30**, 1530010 (2015).
- [49] B. A. Li, W. J. Guo, and Z. Z. Shi, *Phys. Rev. C* **91**, 044601 (2015).
- [50] G. C. Yong, [arXiv:1503.08523](https://arxiv.org/abs/1503.08523).